JOURNAL OF MATERIALS SCIENCE 10 (1977) 1176–1184

The deformation and fracture behaviour of glass-filled ABS

I.R. DOVER, I.O. SMITH, G.A. CHADWICK
Department of Mining and Metallurgical Engineering, University of Queensland, St. Lucia 4067, Queensland, Australia

The tensile and fracture characteristics of pigmented ABS containing 30 wt % rubber reinforced with 30 wt % glass fibre have been examined over a range of strain-rates extending from approximately 10^{-4} to 10^{-1} sec^{-1} within the temperature range 293 to 353 K. The glass fibre-reinforced composite had significantly increased fracture strength compared with the base polymer but possessed decreased ductility. The marked yield point which is characteristic of the ABS base polymer was absent from the reinforced material. Two different regions were found to exist on the fracture surfaces of composite specimens. One region possessed the characteristics of a weak interfacial bond while the other showed evidence of strong, interfacial bonding. In both regions extensive fibre pull-out was observed. The variation in fracture strength and morphology with strain-rate and temperature of testing is explained in terms of the properties of an interfacial region adjacent to the fibres which possesses viscoelastic properties different from those of the bulk polymer. The effect of adiabatic heating at the crack tip is also taken into account in the high temperature–high strain rate regime.

1. Introduction

Development of theories to explain the behaviour of short-fibre reinforced thermoplastics has been slow because of the large number of parameters which affect the properties of a given composite. The study of injection-moulded fibre/thermoplastic composites must necessarily include the effects of such variables as the dispersion, concentration, orientation and length of the fibres together with the nature of the fibre/matrix interface. It has been noted [1] that for the same moulding conditions, the patterns of fibre dispersion and orientation are reproducible within the composite and are indicative of the polymer melt flow pattern. Fibre/matrix interface adhesion can be varied either by applying a surface treatment to the fibres prior to moulding or by using different combinations of fibres and matrix resins. Speri and Jenkins [2] and Blumentritt *et al.* [3] have shown that the degree of adhesion has a pronounced effect on the morphology of fracture surfaces of fibre composite materials. These studies revealed that fracture occurred primarily by fibres pulling out of the matrix resin in both ductile and brittle composites and for good and poor interfacial strengths. No strain-rate effects of fracture morphology were reported, presumably implying a unique fracture morphology for each composite couple.

The tensile deformation behaviour of some short-fibre reinforced thermoplastics has been studied [4–6] and some general characteristics have become known. Addition of the reinforcement significantly raises the ultimate strength and modulus of the composite as compared to the unfilled matrix resin, but markedly decreases its elongation to failure. Although much work has been done on the effect of strain-rate and temperature on the behaviour of unfilled polymers, similar studies on fibre composites have been few, and it was with this purpose in mind that the present investigation on a glass-fibre reinforced ABS was initiated.

© *1977 Chapman and Hall Ltd. Printed in Great Britain.*

2. Experimental

2.1. Materials

The thermoplastic resin used as the matrix material was a Cycolac brand pigmented ABS with a rubber content of 30 wt %. Tensile specimens with a glass fibre content of 30 wt % were commercially injection-moulded to a shape specified by ASTM D647 having a parallel gauge length of 50 mm and a cross-section of 12.7 mm by 3.2 mm from feedstock consisting of a mixture of ABS pellets and glass fibres. The original fibre length was 6.4 mm and the fibre diameters lay between 12 and 15 μm.

2.2. Tensile tests

Tensile tests were performed at four temperatures, 293, 313, 333 and 353 K over a range of strain-rates from approximately 10^{-4} to 10^{-1} sec^{-1}. All testing was conducted on an Instron 1026 testing machine with constant cross-head speeds ranging from 0.05 to 500 mm min^{-1}, the strain-rates being calculated from the cross-head speeds. For the elevated temperature tests, a chamber which circulated hot air was fitted to the Instron machine; the temperature of the air was controllable to less than $\pm$ 1 K about the set temperature and the specimen temperature was monitored by two thermocouples attached to either end of the gauge length.

Qualitative studies of the fracture properties of the composite utilized a number of thin tensile specimens. These were manually prepared from the standard specimens by grinding and polishing operations down to a minimum thickness of approximately 0.5 mm. Tensile fracture surfaces of the standard test specimens and the surfaces of polished, deformed, thin tensile specimens were examined by scanning electron microscopy after coating with a layer of vacuum deposited aluminium.

To further investigate the fracture characteristics of the material, a series of notched tensile tests were conducted over the range of cross-head rates available at 293 and 333 K. Standard ASTM D647 tensile test pieces were notched on one side of the gauge length with a slot which was 0.4 mm wide and had a tip radius of curvature of 0.2 mm. The notch length was such to remove 32% of the gauge area. The fracture surfaces of these notched samples were examined by scanning electron microscopy after coating with aluminium.

3. Results

3.1. Fibre arrangement

The end-gated moulds produced tensile specimens whose fibres were reasonably well aligned along the direction of the gauge length. There was in all cases, however, a region of maximum dimensions 5 mm by 0.5 mm in the centre of the cross-section and following the gauge length wherein the fibres were misaligned to the degree that many lay perpendicular to the gauge length. The extent of this region could be readily determined by eye or by low magnification optical microscopy as it appeared white when metallographically prepared [7]. No attempt was made to ascertain the cause of this misalignment.

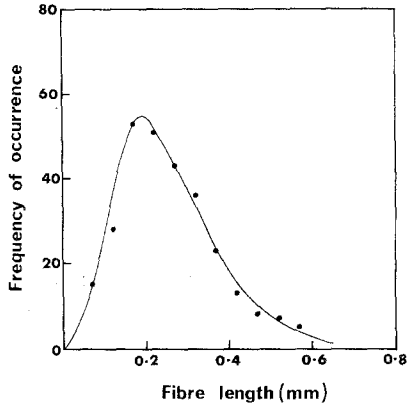

Figure 1 Distribution of fibre lengths in moulded glass/ABS composites.

The length distribution of the fibres in the present composite was determined by counting fibres collected from a sample whose matrix polymer had been dissolved in acetone. Results of this gave the distribution shown in Fig. 1 in which the average fibre length is slightly over 0.2 mm. It is thus apparent that the commercial moulding techniques unfortunately lead to considerable fibre breakage.

3.2. Tensile behaviour

The typical behaviour of glass-reinforced ABS subjected to a tensile load is shown in Fig. 2. Increasing the temperature at the constant strain-rate of 2.78×10^{-4} sec^{-1} causes a small decrease in the initial modulus and a large decrease in the fracture stress. Fracture occurred at elongations generally between 3 and 4% for all combinations

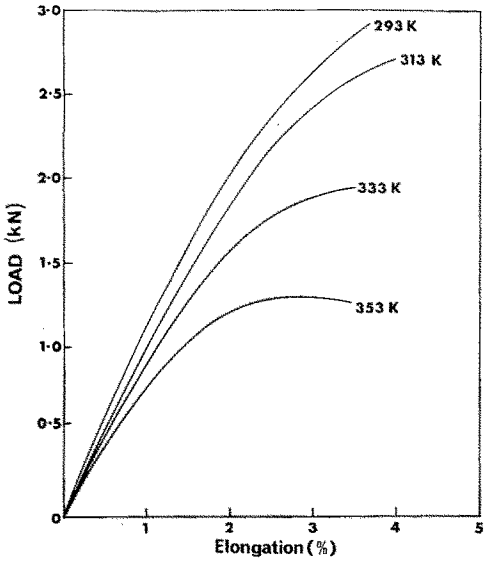

Figure 2 Load–elongation curves obtained in tensile testing glass-reinforced ABS at a strain-rate of 2.8×10^{-4} sec^{-1} at four temperatures.

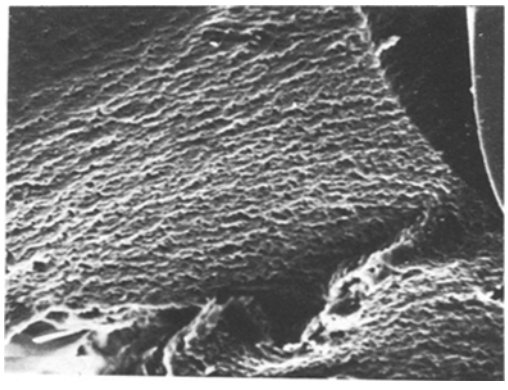

Figure 3 Scanning electron micrograph of the deformed surface of a thin tensile specimen showing the voiding which accompanies the formation of stress-whitened material. A region of undeformed matrix is shown in the lower right-hand corner of the micrograph, × 2000.

of strain-rate and temperature, with no apparent dependence on either of these variables. The unfilled ABS resin exhibits a pronounced yield point at approximately 6% elongation and fails near 20% elongation [8]. Only those speciments tested at 353 K with low rates of strain showed any tendency towards a load decrease prior to fracture.

During each tension test, localized regions of stress whitening appeared on the surface of the specimens at elongations greater than 1%. As the deformation increased, the number and size of these regions continued to grow; their lengths increased by propagation in a direction macroscopically perpendicular to the applied stress. Scanning microscopy of previously polished thin tensile samples was employed to reveal the nature of the deformation in the stress-whitened surface bands. Fig. 3 shows that the stress-whitened regions are collections of tiny voids whose maximum diameters are of the order of 1 to 2 μm. That voiding occurred at the fibre/matrix interface is evident from the view of the surface depression at the lower left of the micrograph where the deformation has caused the matrix material to pull away from the fibre. Generally, the final fracture of the specimen occurred at one of the more prominent stress-whitened bands. Tests performed at high temperatures and low strain-rates proved very valuable in illustrating the macroscopic fracture processes. In the majority of these tests a clearly distinguishable white mark was initiated at a corner of the specimen and this slowly propagated across one of the flat faces until, upon reaching some critical length, catastrophic failure occurred. In other cases, fracture occurred without the initial growth of an observable white mark, implying that the initial deformation was wholly internal.

All fracture surfaces exhibited two distinctive regions, the extent of which could be gauged readily by eye. The first of these was a highly stress-whitened area which was termed the "slow growth" region because it corresponded with the crack-initiation stage prior to catastrophic failure. The second major region of the fracture surface was that which corresponded to the catastrophic failure and has been named the "fast fracture" region. This area exhibited a much lower level of stress whitening.

The effect of strain-rate on the propagation of the brittle crack was seen qualitatively by examination of the fracture surface profile and adjacent regions of the gauge length. At low strain-rates the crack propagated across the specimen as a single defect with little tendency to move out of a plane perpendicular to the applied stress. However, at high strain-rates, there was a pronounced tendency for the crack to branch, as seen by the formation of stress-whitened material, at an angle to the primary crack front. In many cases, bifurcation occurred and one or both of the secondary cracks passed completely through the thickness of the specimen. Fig. 4 shows a bifurcation which resulted in the formation of a wedge of material due to complete propagation

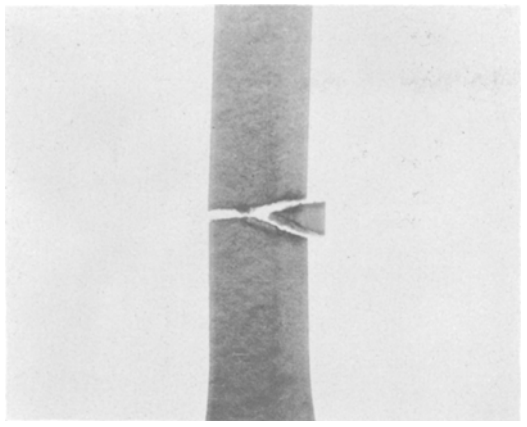

Figure 4 Tensile specimen fractured at a strain-rate of 1.4×10^{-1} sec^{-1} showing branching of the crack during catastrophic failure.

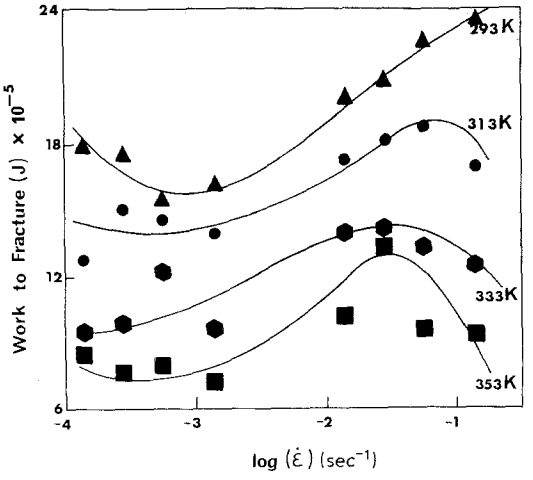

Figure 6 Work to fracture of tensile specimens as a function of strain-rate for the four temperatures of testing.

of both secondary cracks. It was noted that the angle of the initial branching from the plane of the original crack varied from about 20° to 35° with the most common angle being approximately 25°.

The fracture stress was observed to decrease with increasing temperature and decreasing strain-rate. Fig. 5 shows a plot of the fracture stress normalized by the test temperature, σ_{uc}/T, as a function of the logarithm of strain-rate for each of the four-test temperatures. Quite clearly, over most of the strain-rate range, there is a linear

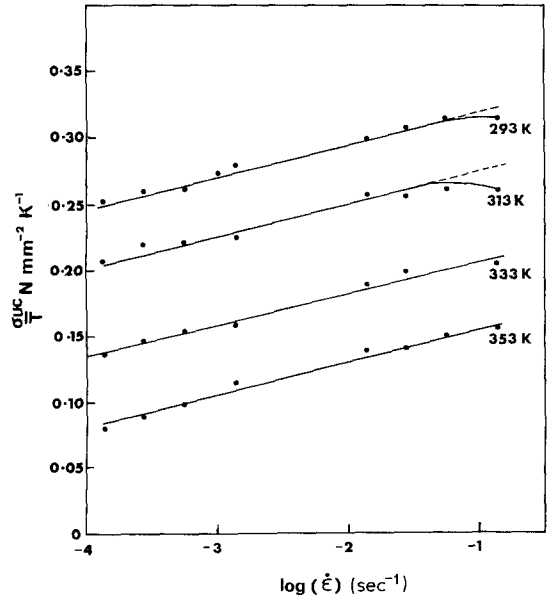

Figure 5 σ_{uc}/T as a function of strain-rate for each of the four temperatures of testing.

relationship between these two variables. However, at low temperatures and at strain-rates exceeding 10^{-1} sec^{-1} there is some deviation from this linear relationship. Unfortunately, the nature of this deviation could not be fully explored since the upper limit of cross-head speed of the Instron machine had been reached.

Fig. 6 shows a plot of the work of fracture of the tensile specimens (i.e. the total area under the load–elongation curve) as a function of the strain-rate for the four test temperatures. Although there is considerable scatter in the results, there are two distinct sections to the set of curves. The peak which separates these sections moves to lower strain-rates as the temperature increases, suggesting that adiabatic heating at the tip of the propagating crack may be important at high strain-rates.

Typical load versus displacement curves obtained in tensile testing the notched samples are presented in Fig. 7. They are characterized by a deviation from linearity at low loads of 100 N, the load level of this initial deviation from linearity increasing systematically with increasing strain-rate. At all but the fastest strain-rate this initial deviation was followed by a region in which the slope of the load versus displacement curve decreased slowly with increasing load until fracture occurred. At the fast cross-head rate of 8.5 mm sec^{-1}, fracture of the sample occurred at a load approximately equal to the initial deviation. The results of the notched tensile tests are summarised in Table I.

It is evident from Table I that the previously described tendency of the fracture stress to deviate

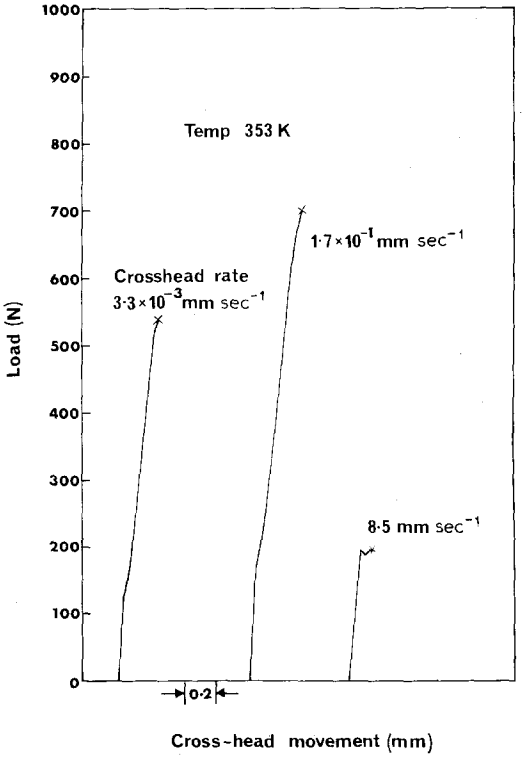

Figure 7 Load-elongation curves obtained in tensile testing of notched samples at 353 K and various cross-head rates.

TABLE I Notched tensile test results

Cross-head rate (mm sec^{-1})	Fracture stress (MN m^{-2})		Notch sensitivity ratio (UTS of notched sample/ UTS of unnotched sample)	
	293K	353K	392K	353K
8.3×10^{-4}	26.2	21.3	0.41	0.57
3.3×10^{-3}	30.5	20.8	0.45	0.50
8.3×10^{-3}	31.4	21.4	0.44	0.48
3.3×10^{-2}	30.8	24.5	0.42	0.48
1.7×10^{-1}	34.7	25.6	0.43	0.45
1.7	26.8	25.9	0.31	0.40
8.5	9.8	7.0	0.11	0.10

from an Eyring relationship toward lower fracture stresses at high strain-rates (Fig. 5) is accentuated by the presence of a notch in the sample. Furthermore, the values of notch sensitivity ratio show that glass-filled ABS is extremely notch sensitive and that this sensitivity increases with increasing strain-rate.

3.3. Fractography

The fracture surfaces of the tensile specimens were covered with a forest of fibres (Fig. 8)

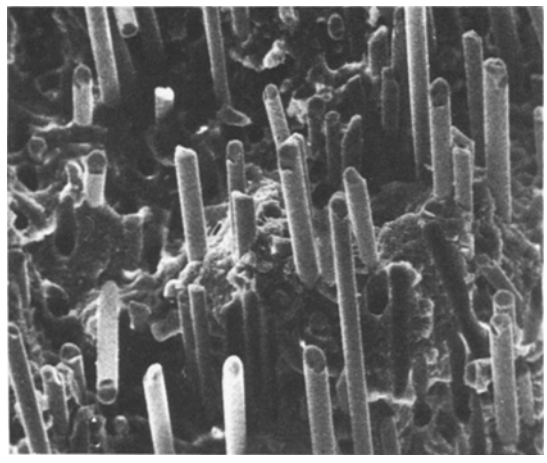

Figure 8 Typical tensile fracture surface in a region of good fibre alignment showing the dominance of fibre pull-out, X 280.

indicating that fibre pull-out was the dominant mechanism of final failure in this composite.

The characteristics of the "slow growth" region are illustrated by the fractograph in Fig. 9. Fibres which pulled out of the matrix were notably free of adhering polymeric material, and a cavity had formed surrounding the locations of fibres, as illustrated in the figure.

Detail of the ABS matrix shows that it has undergone severe drawing about the rubber particles to produce collections of voids [9]. The microstructural characteristics of the fast fracture region are illustrated in Fig. 10. Fibres protruding from the surface are tightly bound by the matrix and some appear dirty due to the clinging of the polymer to their surfaces. More of

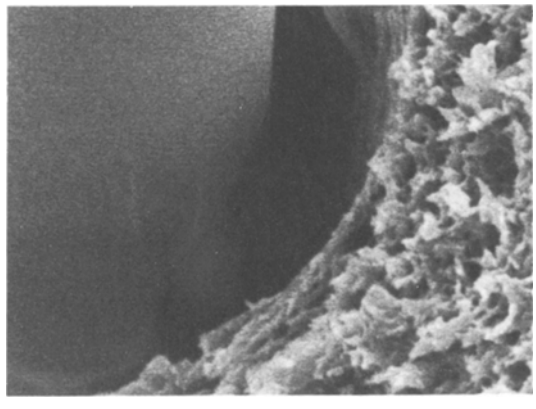

Figure 9 Detail of deformation of the matrix resin within the "slow-growth" region showing the heavily drawn nature of the polymer and debonding of the fibre–matrix interface, X 5000.

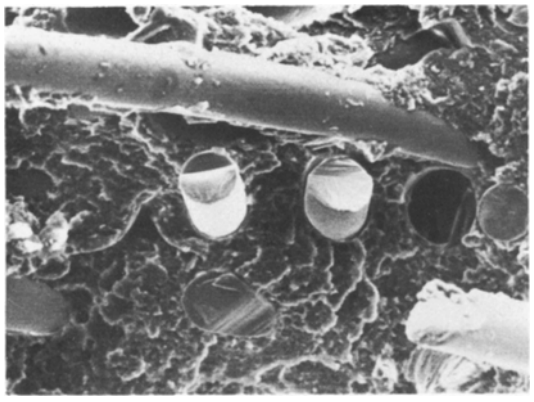

Figure 10 Detail of fracture surface of the material within the region of "fast fracture" showin g the "flaky" nature of the fracture surface and the tight bonding of matrix and fibre, × 1000.

the fibres here were seen to be broken in the plane of the fracture than was evident in the slow growth region. Between the fibres the matrix was extremely rugged and it had adopted a rounded morphology without the incidence of drawing [9].

The macroscopic appearance of the fracture surfaces of the notched tensile samples tested at 293 and 353 K is illustrated in Fig. 11. These fracture surfaces closely resemble those of the parallel-sided tensile specimens in that they exhibit two well-defined regions, an intensely stress-whitened "slow fracture" region near the notch and a relatively unwhitened "fast fracture" region remote from the notch. There was a systematic increase in the amount of white, "slow fracture" surface with increasing temperature and decreasing strain-rate. The detail of the fracture surfaces in the slow and fast growth regions closely resembled those of the corresponding regions in the parallel-sided samples shown in Figs. 8 to 10.

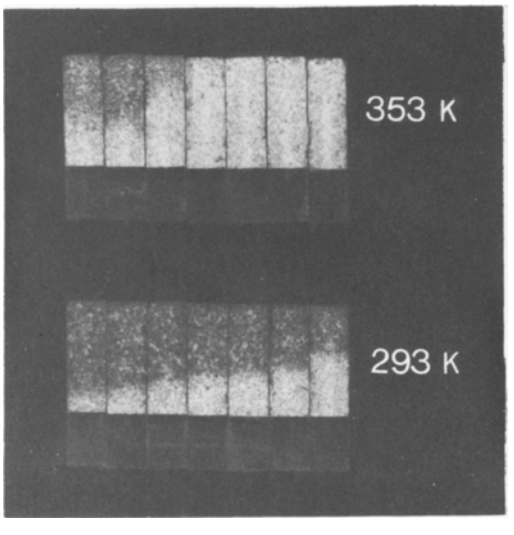

Figure 11 Macroscopic appearance of the fracture surface of the notched tensile specimens tested at 293 and 353K and a range of strain-rates decreasing from left to right.

4. Discussion

The association of stress whitening in polymeric materials with the formation of crazes or random distributions of voids is now generally accepted, and is a view that is supported in the present investigation by the observation of voids in the stress-whitened surface regions of deformed, thin tensile specimens and in the slow growth regions of the fracture surfaces. The formation of obvious crazes as seen by Matsuo [11], Hagerman [12], and Truss and Chadwick [8] in ABS polymer was not detected in the study of this glass/ABS composite. However, the micromorphology of the matrix material in the slow and fast growth regions of the fracture surfaces was similar to that observed by Hagerman [12] and Truss and Chadwick [9] on the fracture surfaces of ABS tensile specimens where fracture occurred in a crazed region.

It has been observed that all fracture surfaces of the glass-filled ABS were characterized by fibre pull-out. The critical fibre length l_c in a fibre composite is given in terms of the fibre fracture stress σ_{uf}, fibre radius r, and interfacial strength τ as

$$l_c = \frac{\sigma_{uf} r}{\tau}.$$

or the purpose of determination of a lower ound value for the critical length, an upper ound value of the shear strength was taken to be ual to the tensile strength of the unfilled matrix]. Using a glass fibre fracture stress of 3725 $N m^{-2}$ [10], values of the critical lengths were lculated to be

$$l_c = 0.6\,\text{mm at } \dot{\epsilon} = 10^{-4}\ \text{sec}^{-1}$$

$$l_c = 0.5\,\text{mm at } \dot{\epsilon} = 10^{-1}\ \text{sec}^{-1}.$$

ence most of the fibres in the composite are low critical length for all testing conditions. his explains the dominance of fibre pull-out at fracture and suggests that very little fibre fracture occurs during deformation of the specimen.

On any single fracture surface, two clearly different regions were observed. In the slow crack growth regime, the matrix showed extensive debonding from the fibre which, from previous work [3], would imply a low strength interfacial bond. On the other hand, the fast fracture regime exhibited no significant debonding around the fibres, implying [3] a higher strength interfacial bond. Since the chemical bond strength obviously does not change within a single specimen, these results require the interfacial bond to possess viscoelastic properties. That this is so can be obtained from the following analysis.

The fact that plots of σ_{uc}/T versus log $(\dot{\epsilon})$ for the composite produce a series of straight parallel lines over the greater portion of the strain-rate range suggests that a rate process is involved in determining the failure of the specimens. Because these results are similar to those obtained for a material whose deformation behaviour is described by the Eyring viscosity equation for a single, thermally activated process, it is possible to determine values for the quantities which correspond to the activation volume v and the activation enthalpy ΔH in the Eyring analysis. It is emphasized, however, that these values are not those of the parameters for the yield behaviour of the matrix resin, in this case ABS, since the values of stress to which the current analysis refers include the contribution of the fibres whose behaviour is purely elastic and so not thermally activated. If these fibres were bonded to the matrix with a bond that behaved elastically, it would be expected that the σ_{uc}/T versus ln $\dot{\epsilon}$ curves of the composite would be displaced to higher stresses but remain at the same slope as the ABS matrix material. Hence the same value of v would be derived. That this is not the case is shown by the data in Fig. 12.

Calculation of the apparent thermodynamic parameters from the data expressed in Fig. 5 yields $v = 1330\,\text{Å}^3$ and $\Delta H = 16.6\,\text{kcal mol}^{-1}$. Truss and Chadwick [7] have performed an Eyring analysis on the yield stress of an ABS polymer similar to that used as the matrix of the present composite, and have determined that for this material, $v = 3175\,\text{Å}^3$ and $\Delta H = 61.5$ kcal mol^{-1}. A possible model which can explain these differences in thermodynamic parameters involves the consideration of an interface of finite thickness in which the nature and/or properties of the polymer are altered. The observed difference in the values of activation volume mentioned above indicates that this interfacial region between fibre and matrix must possess viscoelastic properties. To further examine this phenomenon, calculations were performed on a simple model, in which residual stresses and stress concentrations are neglected, to derive the approximate value of "interfacial" shear strength as a function of strain-rate and temperature. Since the fibres almost all lie below the critical fibre length, a basic rule of mixtures calculation was performed for 15 vol % glass (30 wt %) based on the equation:

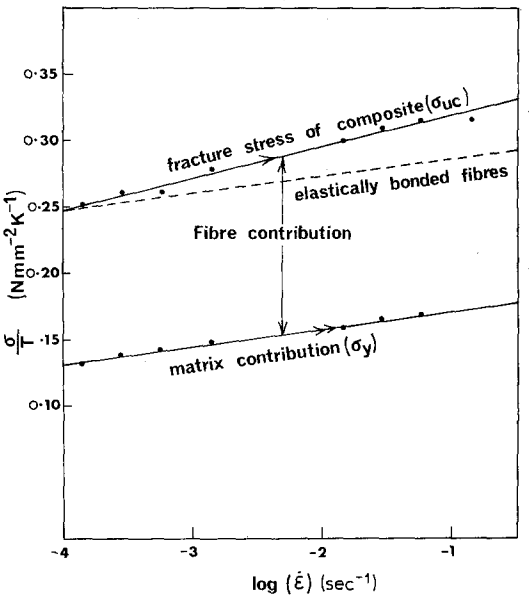

Figure 12 Comparison of Eyring plots for the fracture stress of the glass ABS composite with those for the yield stress of the unfilled ABS (as determined by Truss and Chadwick [7].

$$\sigma_{uc} = 0.85\,\sigma_m + 0.15\,\sigma_f \qquad (1)$$

where σ_{uc} is the composite fracture stress, σ_m the average matrix stress at fracture, and σ_f the average fibre stress at fracture. The average matrix stress at composite fracture was assumed to be the yield stress of the unfilled polymer tested under identical conditions of strain-rate and temperature. With this assumption and the experimental values of composite fracture stress, the average fibre stress was calculated. Following the simple model used by Kelly and Tyson [13], the stress in the fibre was assumed to rise from the fibre end in a linear manner according to

$$\sigma = \frac{\tau x}{r} \qquad x < l_c/2 \qquad (2)$$

where σ is the normal stress in fibre, x the distance from fibre end, r the fibre radius, τ the interfacial shear stress, and l_c the critical fibre length.

In this simple model the average fibre stress for fibres shorter than the critical length is one half of the maximum fibre stress. By substituting the value of maximum fibre stress and one half of the average fibre length into Equation 2, the interfacial shear strength was calculated. The results are summarized in Table II. It is clear that the interfacial shear strength increases with strain-rate and decreases with temperature as would be expected of a visco-elastic material. The general level is about that of the matrix yield strength although the systematic variation of the relationship between interfacial shear strength and matrix yield strength indicates that the bond does possess slightly different activation parameters from the matrix. Determination of these parameters for the interfacial zone gives an activation volume of 2286 Å^3 and an activation enthalpy of 35 kcal mol^{-1}.

TABLE II Calculation of interfacial shear strength

$\dot{\epsilon}$ (sec^{-1})	Temperature (K)	Interfacial shear strength (MN m^{-2})	Fraction of matrix yield strength
10^{-4}	293	34.8	0.84
3×10^{-2}	293	44.8	0.92
10^{-4}	313	32.1	0.99
3×10^{-2}	313	42.0	1.03
10^{-4}	333	23.2	1.05
3×10^{-2}	333	35.9	1.09

The data displayed in Fig. 6 and Table I indicate that both the work to fracture of the parallel sided bars and the fracture stress of the notched specimens initially show a rise with increasing strain-rate followed by a marked decrease. However, the data in Figs. 5 and 7 show that the stress to initiate fast fracture, which can be taken as the fracture stress of the parallel-sided samples and the inflection point in the load–elongation curves for the notched bars, increases with strain-rate. An explanation of these trends can now be given in terms of the preceeding analysis and the competition between the slow and fast fracture processes as well as adiabatic heating.

The initiation of fast fracture in parallel-sided samples requires the growth of the crack by slow growth mechanisms to dimensions sufficient to satisfy a fast fracture criterion. Due to the visco-elastic nature of both the matrix and the interfacial region the slow fracture process would require more stress and hence more energy as the strain-rate is increased. On the other hand, fast strain-rates generate higher stored elastic energy and hence fast fracture requires smaller critical crack dimensions. The interaction of these effects would produce a strain-rate dependence of the initiation stress (of fast fracture) of the type depicted in Figs. 5 and 7 where the rate of increase of this stress is lessened at higher strain-rates. In considering the total work to fracture two effects must be considered. The first of these is the amount of high energy absorption slow fracture which precedes fast fracture; the second is the effects of the adiabatic heating which would occur at the tip of a crack which is rapidly advancing through the sample. The first of these factors would give rise to a fracture energy dependence on strain-rate similar to the initiation stress dependence discussed above. The shape of the curves in Fig. 6 indicates that adiabatic heating has a predominant effect on fracture energy at high strain-rates at high testing temperatures.

5. Conclusions

(1) The addition of 30 wt % short glass fibres to the ductile thermoplastic ABS reduces ductility and eliminates the yield point.

(2) The temperature compensated fracture stress of the composite as a function of the logarithm of the strain-rate generates a series of straight, parallel lines over the greater portion of the strain-rate range. An Eyring analysis based on these results yields an activation enthalpy of 16.6 kcal mol^{-1} and an activation volume of 1330 Å^3.

(3) Two different regions exist on the fracture surfaces of tensile specimens. One region possesses characteristics of a weaker interfacial bond whilst the other shows evidence of stronger interfacial bonding. In all regions, fibre pull-out occurs. The deformation of the composite material involves the formation of voids within the polymer and at the fibre/matrix interface.

(4) An analysis of the strength of the interfacial region indicates that it possesses viscoelastic properties having an apparent activation enthalpy of 35 kcal mol^{-1} and an apparent activation volume of 2286 Å^3.

(5) In the high temperature, high strain-rate regime the energy to fracture the material is significantly decreased by adiabatic heating at the crack tip.

Acknowledgements

We wish to thank Marbon Chemical (Australia) Pty Ltd, for supplying the ABS used in this research, and Fortified Polymers (Sydney) for manufacturing the glass fibre-reinforced specimens.

References

1. J. H. DAVIS, *Plastics and Polymers* **38** (1970) 137.
2. W. M. SPERI and C. F. JENKINS, *Poly. Eng. Sci.* **13** (1973) 409.
3. B. F. BLUMENTRITT, B. T. VU and S. L. COOPER, *Composites* **6** (1975) 105.
4. G. F. HARDY and H. L. WAGNER, *J. Appl. Polymer Sci.* **13** (1969) 961.
5. W. H. BOWYER and M. G. BADER, *J. Mater. Sci.* **7** (1972) 1315.
6. R. M. OGORKIEWICZ and G. W. WEIDMANN, *J. Mech. Eng. Sci.* **16** (1974) 10.
7. M. W. DARLINGTON and G. R. SMITH, *Polymer* **16** (1975) 459.
8. R. W. TRUSS and G. A. CHADWICK, *J. Mater. Sci.* **11** (1976) 111.
9. *Idem., ibid* **11** (1976).
10. D. M. MARSH, Proceedings of the International Conference on Fracture of Solids, Washington (Gordon & Breach, New York, 1962) p. 143.
11. M. MATSUO, *Polymer* **7** (1966) 421.
12. E. M. HAGERMAN, *Polymer Preprints* **15** (1974) 217.
13. A. KELLY and W. R. TYSON, *J. Mech Phys. Solids* **14** (1966) 177.

Received 27 September 1976 and accepted 22 November 1976.